A&A 413, 1029–1036 (2004)
DOI: 10.1051/0004-6361:20034292
© ESO 2004

Astronomy & Astrophysics

ε Indi Ba,Bb: The nearest binary brown dwarf⋆

M. J. McCaughrean[1], L. M. Close[2], R.-D. Scholz[1], R. Lenzen[3], B. Biller[2], W. Brandner[3], M. Hartung[4], and N. Lodieu[1]

[1] Astrophysikalisches Institut Potsdam, An der Sternwarte 16, 14482 Potsdam, Germany
[2] Steward Observatory, University of Arizona, 933 N. Cherry Ave., Tucson, AZ 85721–0065, USA
[3] Max-Planck-Institut für Astronomie, Königstuhl 17, 69117 Heidelberg, Germany
[4] European Southern Observatory, Alonso de Cordova 3107, Vitacura, Santiago, Chile

Received 9 September 2003 / Accepted 2 October 2003

Abstract. We have carried out high angular resolution near-infrared imaging and low-resolution ($R \sim 1000$) spectroscopy of the nearest known brown dwarf, ε Indi B, using the ESO VLT NAOS/CONICA adaptive optics system. We find it to be a close binary (as also noted by Volk et al. 2003), with an angular separation of 0.732 arcsec, corresponding to 2.65 AU at the 3.626 pc distance of the ε Indi system. In our discovery paper (Scholz et al. 2003), we concluded that ε Indi B was a ~50 $M_{\rm Jup}$ T2.5 dwarf: our revised finding is that the two system components (ε Indi Ba and ε Indi Bb) have spectral types of T1 and T6, respectively, and estimated masses of 47 and 28 $M_{\rm Jup}$, respectively, assuming an age of 1.3 Gyr. Errors in the masses are ±10 and ±7 $M_{\rm Jup}$, respectively, dominated by the uncertainty in the age determination (0.8–2 Gyr range). This uniquely well-characterised T dwarf binary system should prove important in the study of low-mass, cool brown dwarfs. The two components are bright and relatively well-resolved: ε Indi B is the only T dwarf binary in which spectra have been obtained for both components. The system has a well-established distance and age. Finally, their orbital motion can be measured on a fairly short timescale (nominal orbital period ~15 yrs), permitting an accurate determination of the true total system mass, helping to calibrate brown dwarf evolutionary models.

Key words. astrometry – surveys – stars: late-type – stars: low mass, brown dwarfs – stars: binaries: general

1. Introduction

Binary systems are a common product of the star formation process and there is no reason to suspect that the same would not hold below the hydrogen-burning limit, in the domain of brown dwarfs. Binary systems offer important advantages in studies of the characteristics of brown dwarfs, in part because the two components are expected to be coeval and have the same chemical composition. The differential measurement of physical parameters such as luminosity, effective temperature, and surface gravity would then provide crucial constraints on evolutionary models. Furthermore, sufficiently tight binary systems would allow the direct measurement of the system mass via the monitoring of orbital motion.

After a number of unsuccessful searches, the first spatially-resolved brown dwarf binary was found in the solar neighbourhood by Martín et al. (1999) and, subsequently, high spatial resolution imaging has identified a significant number of such systems (e.g., Close et al. 2002a; Goto et al. 2002; Potter et al. 2002; Gizis et al. 2003; Close et al. 2003). Indeed, roughly 20% of a magnitude-limited sample of ~135 L dwarfs and 10 T dwarfs imaged with the HST have been shown to have candidate companions at projected separations of 1–10 AU (Reid et al. 2001; Bouy et al. 2003; Burgasser et al. 2003). Many of these sources have since been confirmed as physical pairs with second epoch data.

Particularly important among brown dwarfs are those with well-established distances and ages, as their physical parameters can be accurately determined and they can be used as key templates in the understanding of the physical evolution of these substellar sources (e.g., Gl 229 B: Nakajima et al. 1995; Gl 570 D: Burgasser et al. 2000). An especially rewarding discovery would be a binary brown dwarf system with a well-established distance and age, a small separation such that its orbit could be measured on a reasonable timescale, and yet nearby enough that its components would be bright, well-resolved, and thus readily amenable to observations.

Scholz et al. (2003; hereafter SMLK03) recently reported the discovery of a new benchmark brown dwarf, ε Indi B, as a very wide (~1500 AU) companion to the nearby, very high proper-motion (~4.7 arcsec/yr) southern star, ε Indi A. With an accurate Hipparcos distance to the system of 3.626 pc (ESA 1997), ε Indi B was the nearest known brown dwarf to the Sun and the brightest member of the T dwarf class by roughly 2 mag in the near-IR. In addition, through its association with

Send offprint requests to: M. J. McCaughrean, e-mail: mjm@aip.de
⋆ Based on observations collected with the ESO VLT, Paranal, Chile.

Article published by EDP Sciences and available at http://www.aanda.org or http://dx.doi.org/10.1051/0004-6361:20034292

ε Indi A, it had a reasonably well-determined age of ∼1.3 Gyr (likely range 0.8–2 Gyr; Lachaume et al. 1999). This fortuitous combination of parameters made it a thus far unique object for detailed, high precision studies; in particular, high resolution spectroscopy of its atmosphere could be important as, with a spectral type of T2.5, it was one of the few objects in the transition zone between L and T dwarfs where dramatic changes in the atmospheric properties are known to occur.

Another exciting prospect raised by the discovery of ε Indi B was that deep, high angular resolution imaging might reveal lower-mass companions, potentially even into the planetary domain, at separations small enough (∼1 AU) that the orbit could be traced out in only a few years, leading to an accurate, model-independent determination of the total system mass.

We observed ε Indi B with the NAOS/CONICA (henceforth NACO) near-IR adaptive optics system on UT4 (Yepun) of the ESO VLT, Paranal, Chile, on August 13 2003 (UT). It was readily resolved into two components (henceforth ε Indi Ba and ε Indi Bb following the IAU-approved Washington Multiplicity Catalog nomenclature of Hartkopf & Mason 2003), as also noted five days later by observers at the Gemini-South telescope (Volk et al. 2003). Here we present the first ∼0.1 arcsec resolution near-IR imaging and spectroscopy of the ε Indi Ba,Bb system, from which we determine accurate positions and spectral types for the two components. We then derive effective temperatures and luminosities, and make estimates of the masses based on evolutionary models.

2. Imaging observations

Adaptive optics imaging observations of low-mass stars and brown dwarfs generally use the source itself for self-guiding and correction (cf. observations of L dwarfs by Close et al. 2003). However, as a T dwarf, ε Indi B presents a real challenge to adaptive optics. Despite its proximity, it is a very cool, low-luminosity object and too faint in the optical ($I \sim 17^{\rm m}$) for accurate wavefront sensing. Fortunately though, it is significantly brighter in the near-IR ($K \sim 11^{\rm m}$) and thus perfectly suited to the unique infrared wavefront sensing capability (IR WFS) of the NACO system (Lenzen et al. 2003; Lagrange et al. 2003).

At the time of our observations, the natural seeing was a very good ∼0.5 arcsec FWHM. To further ensure the best possible image correction, we used the N90C10 dichroic in NACO, which sends just 10% of the source flux to the science camera, while diverting the remaining 90% to the IR WFS, which was run in 49 subaperture mode. Combined, these factors enabled us to obtain the sharpest ever (0.08 arcsec FWHM at 2 μm) infrared images of a binary T dwarf.

Standard near-IR AO observing procedures were followed. In each of the J, H, and $K_{\rm s}$ broad-band images, a total of 18 spatially dithered (∼3 arcsec) images were obtained, each with a 5 s integration time. The S27 camera was used with an image scale of 27.07 ± 0.05 milliarcsec/pixel and a total field-of-view of 27.7 × 27.7 arcsec. The VLT derotator maintained north along the Y-axis of the science detector to within 0.06 ± 0.143° throughout. Sky subtraction, flat-fielding, cross-correlation, and image alignment to within 0.01 pixels were carried out using custom scripts (Close et al. 2002a,b) and standard IRAF programs. The total integration time in each filter was 90 s and the final FWHM was 0.116, 0.100, and 0.084 arcsec at J, H, and $K_{\rm s}$, respectively.

Table 1. Relative astrometry and photometry for ε Indi Ba and ε Indi Bb. The image scale in the NACO S27 camera was measured as 27.07 ± 0.05 mas/pixel during NACO commissioning using astrometric binaries and Galactic Centre imaging. The system position angle offset was measured using images taken of the astrometric binary WDS 19043−2132 on August 13 in the same camera configuration: the error in the determination was ±0.143°. The separation and position angle were confirmed in independent data taken in another NACO mode, for which the image scale was measured using both WDS 19043−2132 and a non-astronomical opto-mechanical setup. The errors in the mean separation and position angle include the NACO data measurement errors and the errors in the system parameters. Differential magnitudes measured by Volk et al. (2003) and Smith et al. (2003) at other wavelengths are also given for convenience.

Separation (arcsec)	
J	0.733
H	0.732
$K_{\rm s}$	0.731
mean	0.732 ± 0.002
Position angle (° E of N)	
J	136.81
H	136.78
$K_{\rm s}$	136.83
mean	136.81 ± 0.14
Δ mag (Bb − Ba) (NACO)	
J	$0\overset{\rm m}{.}94 \pm 0\overset{\rm m}{.}02$
H	$1\overset{\rm m}{.}76 \pm 0\overset{\rm m}{.}02$
$K_{\rm s}$	$2\overset{\rm m}{.}18 \pm 0\overset{\rm m}{.}03$
Δ mag (Volk et al. 2003)	
I	$1\overset{\rm m}{.}5$
1.083 μm	$0\overset{\rm m}{.}69$
1.282 μm	$0\overset{\rm m}{.}47$
1.556 μm	$1\overset{\rm m}{.}34$
2.106 μm	$1\overset{\rm m}{.}92$
2.321 μm	$>3\overset{\rm m}{.}8$
Δ mag (Smith et al. 2003)	
1.647 μm	$1\overset{\rm m}{.}9$
2.321 μm	$>3^{\rm m}$

The resulting images are shown in Fig. 1: the new, fainter source, ε Indi Bb, is well resolved for the first time from ε Indi Ba, and is relatively bluer. The rest of the NACO field is empty to a limiting magnitude ∼$3^{\rm m}$ fainter than ε Indi Bb, immediately suggesting that they constitute a physical pair. Volk et al. (2003) checked the 1999.9 epoch 2MASS survey images at the coordinate where the fast-moving ε Indi Ba was located at the 2003.6 epoch of their Gemini-South observations. They found no source with the characteristics of ε Indi Bb, and thus concluded that the two sources must be comoving. Finally, we have checked some short, 0.6 arcsec FWHM seeing VLT FORS1 optical acquisition images taken of ε Indi B on June 2003 which also in retrospect show the source to be binary. The separation and position angle of the system were measured to be 0.57 ± 0.08 arcsec and 139.5 ± 2.6°, respectively, i.e., close to the parameters measured from the NACO images (Table 1).

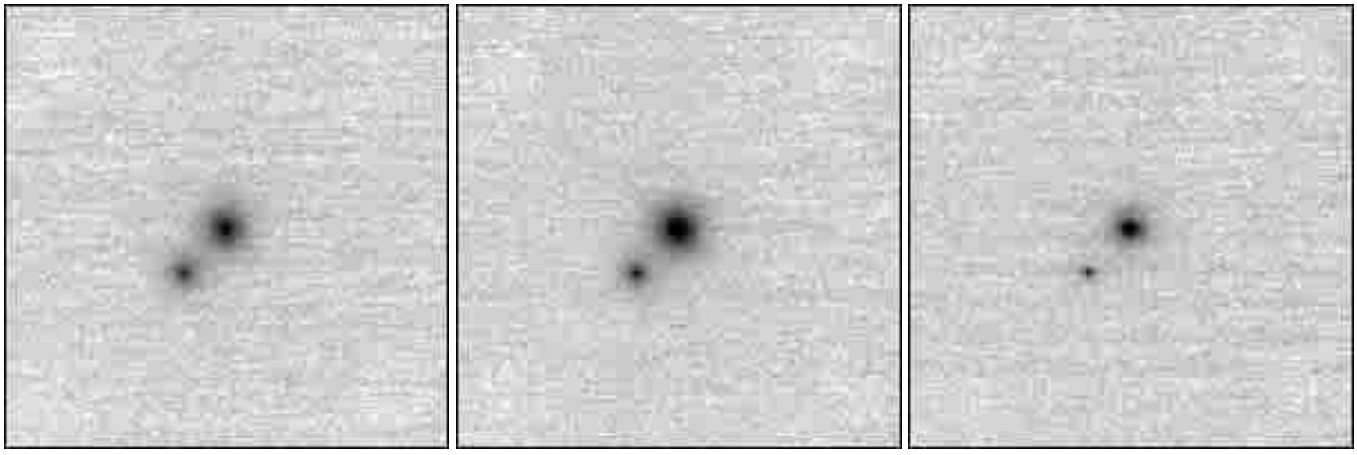

Fig. 1. NACO broad-band near-IR adaptive optics images of the ε Indi Ba,Bb system, with J, H, and K_s from left to right. Each image is a 5.4×5.4 arcsec (19.6×19.6 AU at 3.626 pc) subsection of the full 27.7×27.7 arcsec NACO S27 camera field-of-view. The angular resolutions are ~116, 100, and 84 mas FWHM at J, H, and K_s, respectively. North is up, East left: ε Indi Bb is the fainter source to the south-east. The intensities are displayed logarithmically. No other sources are detected in any filter across the whole NACO FOV.

Due to its very high proper motion, ε Indi B moved 0.8 arcsec in those two months: the separation and PA could not have remained constant unless ε Indi Bb is a comoving, physical companion to ε Indi Ba.

PSF-fitting photometry techniques (IRAF DAOPHOT) were used to measure the relative positions, position angle, and fluxes in all three filters (Table 1). The mean separation of 0.732 ± 0.002 arcsec at the distance of 3.626 ± 0.01 pc distance of ε Indi Ba,Bb (SMLK03) corresponds to a projected spatial separation of 2.65 ± 0.01 AU.

Table 2 lists optical/near-IR photometry and positional data for the system taken from archival photographic plates, the 2MASS and DENIS near-IR sky surveys. There is good agreement between the three K_s/K band magnitudes, but there is a relatively large difference (~$0\overset{m}{.}2$) between the 2MASS Point Source Catalog (2MPSC) and DENIS J magnitudes, and between the 2MPSC and 2MASS Quick Look Atlas (2MQLA) magnitudes derived independently by SMLK03 using M dwarfs for calibration. Also, the 2MPSC H magnitude ~$0\overset{m}{.}3$ is brighter than that derived from the 2MQLA by SMLK03.

Although the 2MPSC and 2MQLA magnitudes are, in principle, derived from the same source data, there are calibration issues with the Quick Look Atlas data that may be responsible for the differences. Equally, it is well known that there are often significant differences in the photometry of T dwarfs obtained in various filter systems, due to the strong molecular absorption bands in their spectra (Stephens & Leggett 2004). In addition, variability is known to occur in T dwarfs (cf. Artigau et al. 2003).

Thus for present purposes, we adopt the 2MPSC magnitudes on the simple grounds that good colour transformations between 2MASS and other photometric systems are readily available (Cutri et al. 2003) and, in particular, have recently been determined for L and T dwarfs explicitly (Stephens & Leggett 2004). The 2MPSC magnitudes are given in Table 3, along with the magnitudes for the individual components, derived using the NACO differential measurements from Table 1 and assuming that the NACO and 2MASS JHK_s colour systems are identical for present purposes.

Table 2. Astrometry and photometry for the combined ε Indi Ba,Bb system from the SuperCOSMOS Sky Surveys based on ESO Schmidt (SSS-ESO) and UK Schmidt (SSS-UK) photographic plates (Hambly et al. 2001a,b), the 2MASS Quick Look Atlas (2MQLA; SMLK03), the 2MASS Point Source Catalog (2MPSC; Cutri et al. 2003), the DENIS second data release (`http://vizier.u-strasbg.fr/viz-bin/Cat?B/denis`), and a public VLT FORS1 I band acquisition image from another group (Ménard, Delfosse, & Monin; ESO program 72.C-0575(A)).

α, δ (J2000.0)		Epoch	Magnitude	Data
22 04 03.113	−56 46 19.46	1984.555	$R = 20.75$	SSS-ESO
22 04 09.465	−56 46 52.58	1997.771	$I = 16.59$	SSS-UK
22 04 10.392	−56 46 57.29	1999.666	$I = 16.77$	SSS-UK
22 04 10.52	−56 46 57.8	1999.855	$J = 12.11$	2MQLA
			$H = 11.59$	2MQLA
			$K_s = 11.17$	2MQLA
22 04 10.52	−56 46 57.7	1999.855	$J = 11.91$	2MPSC
			$H = 11.31$	2MPSC
			$K_s = 11.21$	2MPSC
22 04 10.97	−56 47 00.4	2000.781	$I = 16.90$	DENIS
			$J = 12.18$	DENIS
			$K = 11.16$	DENIS
22 04 12.278	−56 47 06.58	2003.488		FORS1

Table 3. Adopted near-IR magnitudes for the combined ε Indi Ba,Bb system from the 2MASS Point Source Catalog (Cutri et al. 2003) and the derived individual magnitudes for the two components. The NACO and 2MASS JHK_s colour systems are assumed to be identical for this exercise.

Filter	System	Combined	ε Indi Ba	ε Indi Bb
J	2MASS	$11\overset{m}{.}91$	$12\overset{m}{.}29$	$13\overset{m}{.}23$
H	2MASS	$11\overset{m}{.}31$	$11\overset{m}{.}51$	$13\overset{m}{.}27$
K_s	2MASS	$11\overset{m}{.}21$	$11\overset{m}{.}35$	$13\overset{m}{.}53$

Finally, a more detailed analysis of the additional optical and IR survey data allows us to determine a more refined proper

Table 4. Proper motions for ε Indi Ba,Bb and ε Indi A in mas/yr.

Object	$\mu_\alpha \cos\delta$	μ_δ	Source
ε Indi Ba,Bb	+4131 ± 71	−2489 ± 25	SMLK03
ε Indi Ba,Bb	+3976 ± 13	−2500 ± 14	This paper
ε Indi A	+3961.41 ± 0.57	−2538.33 ± 0.40	ESA (1997)

motion for the combined ε Indi Ba,Bb system: it is now much more consistent with that known for the bright primary star, ε Indi A (Table 4). The remaining difference of ∼ 40 mas/yr is consistent with the expected differential motion due to orbital motion of ε Indi Ba,Bb around ε Indi A: if the 1459 AU projected separation corresponds to an orbit lying in the plane of the sky, the maximum differential proper motion between ε Indi A and ε Indi Ba,Bb would be ∼ 39 mas/yr.

3. Spectroscopic observations

Following the direct imaging, NACO was used in long slit grism mode to obtain $R \sim 1000$ classification spectroscopy in the H band (mode S54_3_H, nominal coverage 1.5–1.85 μm, 6.8 Å/pixel dispersion, S54 camera with 54.3 mas/pixel). By turning the instrument rotator, both sources were placed on the slit simultaneously and 12×2 min exposures were made, dithering to different locations along the slit between exposures, for a total on-source integration time of 24 min.

For the spectroscopic observations, the NACO K dichroic was used to send full H band flux to the science detector and just the K band flux to the IR WFS. This choice maximised the signal-to-noise in the spectra but reduced the number of photons available to the IR WFS by roughly 60% compared to the imaging. As a result, the adaptive optics correction was poorer, yielding a spatial resolution of typically 0.3 arcsec FWHM. However, this was nevertheless adequate to ensure well-separated spectra for the two components of the 0.732 arcsec binary.

Observations were also made of the nearby star HD209552 (G2V) shortly afterwards in order to measure the telluric absorption. Tungsten-illuminated spectral dome flats were taken in the same configuration at the end of the night.

Data reduction was standard, employing the IRAF long-slit spectroscopy packages. For each source spectral image, several (typically three) other images with the sources at different locations were combined to make a clean sky image which was subtracted to remove the OH airglow emission. The image was then divided by the spectral dome flat. Then returning to the raw data, the OH lines and the source spectra were traced in order to determine the geometric transformation which linearised the dispersion, placed the OH lines horizontally along rows, and the source spectra vertically down columns. This transformation was applied to all 12 sky-subtracted, flat-fielded images, which were then aligned and co-added with intensity weighting.

Individual spectra for ε Indi Ba and ε Indi Bb were then optimally extracted. By careful measurement of the spatial FWHM along the spectra, it was possible to assess the spectral crosstalk as ∼2.5%, i.e., at the spatial location of ε Indi Bb, the flux of ε Indi Ba is reduced to 2.5% of the flux at its spatial location, and vice versa. At the wavelength of maximum contrast between the two sources, the brighter source ε Indi Ba adds roughly 30% to the flux of the fainter ε Indi Bb, although more typically it is below 10%. Thus in order to remove most of the crosstalk, an appropriately scaled version of the ε Indi Ba spectrum was subtracted from the ε Indi Bb spectrum and vice versa.

Table 5. Near-IR H band spectral classification indices for ε Indi Ba and ε Indi Bb following the schemes of Geballe et al. (2002) and Burgasser et al. (2002).

Index	ε Indi Ba		ε Indi Bb	
	Value	Spectral Type	Value	Spectral Type
Geballe et al. (2002)				
H_2O 1.5 μm	2.01	T0	3.66	T4
CH_4 1.6 μm	1.11	T1	3.27	T6
Burgasser et al. (2002)				
H_2O_B	0.80	T1	5.29	T5
CH_4_B	1.34	T1	6.02	T6

Finally, the two source spectra were divided by the spectrum of the atmospheric calibrator, similarly reduced and extracted, and then multiplied back by a template solar spectrum (Maiolino et al. 1996) smoothed to the resolution of the NACO spectra (∼17 Å FWHM, $R \sim 1000$). Flux calibration was achieved using the H band magnitude given for ε Indi Ba in Table 3 and using the 2MASS H filter profile.

The resulting spectra are shown in Fig. 2, with the major H_2O and CH_4 absorption bands marked. A more detailed analysis is postponed to a future paper, when we should also have higher-resolution spectra covering the entire near-IR, but here we simply use the spectra to provide spectral classifications using the indices of Burgasser et al. (2002) and Geballe et al. (2002). In both systems, the H band contains two indices, one measuring the 1.5 μm H_2O band, the other the 1.6–1.7 μm CH_4 band, and Table 5 gives the values and correspondingly derived spectral types for the two sources. The two Burgasser et al. (2002) indices and the Geballe et al. (2002) CH_4 index all give relatively consistent spectral types of T1 ± 0.5 and T6 ± 0.5 for ε Indi Ba and ε Indi Bb, respectively, while the Geballe et al. H_2O index yields T0 and T4. It is worth noting that this index yields a spectral type of T4.5 for Gl 229 B, while it is more commonly thought of as ∼T6 based on a broader range of indices (Burgasser et al. 2002; Geballe et al. 2002). Thus, for present purposes we assign spectral types of T1 and T6 to the two components of the ε Indi Ba,Bb system.

4. Revised physical properties

With the individual magnitudes and spectral types, along with the accurate distance and relatively well-determined age of the ε Indi Ba,Bb system, we are now able to estimate their physical parameters, as summarised in Table 7.

To begin with, we transform the near-IR photometry for the two components (Table 3) from the 2MASS photometric system to the MKO-NIR system, as the latter is a widely-used standard which is particularly immune to variations due to

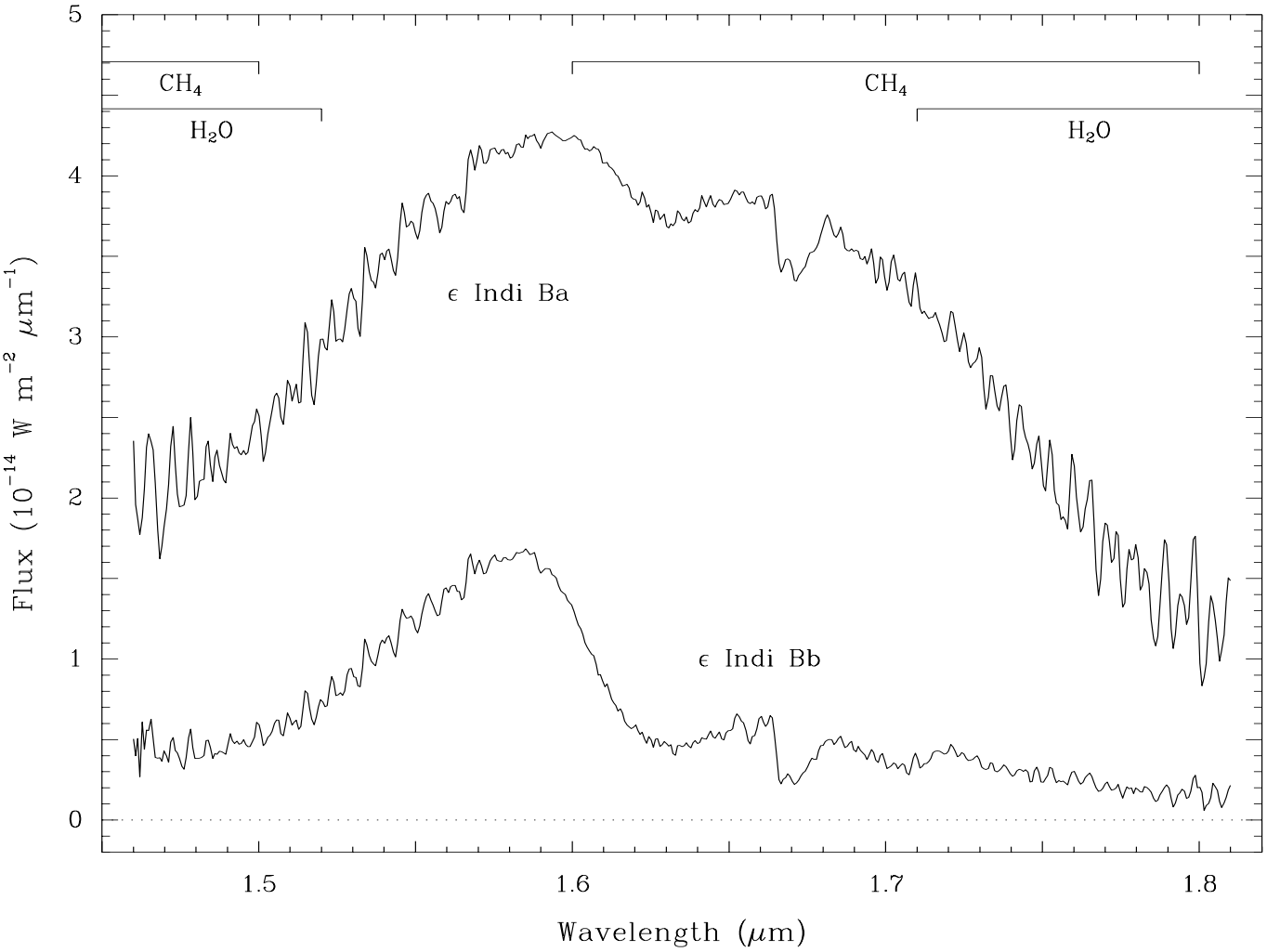

Fig. 2. *H* band spectra of ε Indi Ba and ε Indi Bb. The spectral resolution is ~17 Å FWHM, yielding $R \sim 1000$. Flux calibration was made by convolving the spectrum of ε Indi Ba with the 2MASS *H* filter profile and assuming a 2MASS magnitude of $H = 11\overset{\mathrm{m}}{.}51$ as given in Table 3. The excellent signal-to-noise of the spectra is seen in the relatively smooth 1.58–1.62 μm range; the "ripples" shortward of 1.56 μm and longward of 1.72 μm are real features, predominantly due to H_2O and CH_4 (cf. Geballe et al. 2001; Leggett et al. 2002; McLean et al. 2003; Cushing et al. personal communication), but also possibly in part due to FeH (cf. Cushing et al. 2003). The deep double CH_4 absorption trough seen in both sources at 1.67 μm is also seen in the T6 dwarf Gl 229 B (Geballe et al. 1996), as is the adjacent absorption feature at 1.658 μm seen in ε Indi Bb.

the Earth's atmosphere. Also, importantly, Stephens & Leggett (2004) have recently determined a set of transformations to the MKO system explicitly for L and T dwarfs, which require special attention due to their highly-structured atmospheres. The transformations are parameterised as a function of the spectral type: assuming T1 and T6 for ε Indi Ba and ε Indi Bb, respectively, as determined from our spectra, the resulting magnitudes are given in Table 6. Colours are also given and are seen to be quite consistent with the corresponding spectral types when compared with the compilation of M, L, and T dwarf colours in the MKO system plotted in Fig. 5 of Leggett et al. (2002).

Next, with the magnitudes in the MKO system, we can use the bolometric corrections in that system as determined for late-M, L, and T dwarfs by Golimowski et al. (2004), which are again parameterised as a function of spectral type. This parameterisation yields $BC_K = 2\overset{\mathrm{m}}{.}88$ and $2\overset{\mathrm{m}}{.}22$ for the spectral types T1 and T6 of ε Indi Ba and ε Indi Bb, respectively. For comparison, the online data of Reid (`www-int.stsci.edu/~inr/ldwarf2.html`) give $BC_K = 3\overset{\mathrm{m}}{.}3$ and $2\overset{\mathrm{m}}{.}1$ for spectral types T1 and T6, respectively.

Table 6. Transformed near-IR magnitudes and colours for the two components of the ε Indi Ba,Bb system, using the spectral-type based parameterisation of Stephens & Leggett (2004) to transform between the 2MASS and MKO systems, and assuming T1 and T6 for ε Indi Ba and ε Indi Bb, respectively.

Filter	System	ε Indi Ba	ε Indi Bb
J	MKO	$12\overset{\mathrm{m}}{.}10$	$12\overset{\mathrm{m}}{.}94$
H	MKO	$11\overset{\mathrm{m}}{.}56$	$13\overset{\mathrm{m}}{.}31$
K	MKO	$11\overset{\mathrm{m}}{.}38$	$13\overset{\mathrm{m}}{.}65$
$(J-H)$	MKO	$0\overset{\mathrm{m}}{.}54$	$-0\overset{\mathrm{m}}{.}37$
$(H-K)$	MKO	$0\overset{\mathrm{m}}{.}18$	$-0\overset{\mathrm{m}}{.}34$
$(J-K)$	MKO	$0\overset{\mathrm{m}}{.}72$	$-0\overset{\mathrm{m}}{.}71$

Table 7. Physical parameters for the two components of the ε Indi Ba,Bb system derived using the COND models of Baraffe et al. (2003) covering the plausible range of ages (0.8, 1.3, and 2.0 Gyr) for the system (Lachaume et al. 1999; SMLK03). See text for a detailed discussion of the derivation and the errors in the assumptions, as well as the masses derived in similar fashion from the Burrows et al. (1997) models.

Source	M_K	BC_K	$M_{\rm bol}$	$\log L/L_\odot$	Mass $M_{\rm Jup}$			Radius $R/R_\odot$			$T_{\rm eff}$ K		
					0.8	1.3	2.0	0.8	1.3	2.0	0.8	1.3	2.0
ε Indi Ba	$13\overset{\rm m}{.}58$	$2\overset{\rm m}{.}88$	$16\overset{\rm m}{.}46$	−4.71	38	47	57	0.096	0.091	0.086	1238	1276	1312
ε Indi Bb	$15\overset{\rm m}{.}85$	$2\overset{\rm m}{.}22$	$18\overset{\rm m}{.}07$	−5.35	22	28	35	0.101	0.096	0.092	835	854	875

The differences are probably due in part to the differing photometric systems, but also to some extent to the paucity of T dwarfs with well-determined distances: along with the samples of T dwarfs measured in infrared parallax programs (Tinney et al. 2003), ε Indi Ba and ε Indi Bb will prove important additions once their thermal-infrared magnitudes have been measured.

Applying the Golimowski et al. (2004) bolometric corrections and the distance modulus of $-2\overset{\rm m}{.}20$, we then derive $M_{\rm bol} = 16\overset{\rm m}{.}46$ and $18\overset{\rm m}{.}07$ for ε Indi Ba and ε Indi Bb, respectively. Assuming $M_{\rm bol} = 4\overset{\rm m}{.}69$ for the Sun, we then obtain $\log L/L_\odot = -4.71$ and –5.35 for ε Indi Ba and ε Indi Bb, respectively. The errors in this derivation include those in the NACO and 2MASS photometry, the 2MASS–MKO colour equations, and the distance estimation, but are dominated by the uncertainty in the bolometric corrections. Following SMLK03, we adopt a cumulative error of ±20% in our luminosity determinations.

In SMLK03, we followed the same procedure to this point for ε Indi B and then derived $T_{\rm eff}$ by assuming a radius determined from a relationship between $R/R_\odot$ and $M_{\rm bol}$ given by Dahn et al. (2002) and modified by Reid. That relationship was derived from the evolutionary models of the Lyon (Chabrier et al. 2000) and Arizona (Burrows et al. 1997) groups for L dwarfs at ∼3 Gyr and $M_{\rm bol} = 12^{\rm m}$–$16\overset{\rm m}{.}5$ and predicts a slightly decreasing radius with decreasing luminosity. However, ε Indi Ba and ε Indi Bb are younger T dwarfs with $M_{\rm bol} > 16\overset{\rm m}{.}5$ and, importantly, lie in a domain where the models predict an *increase* in radius with decreasing luminosity due to electron degeneracy pressure support.

Therefore here, we use the Baraffe et al. (2003) models to extract the radii for the luminosities and ages appropriate for the ε Indi Ba,Bb system, and thence the effective temperatures. As discussed in SMLK03, Lachaume et al. (1999) proposed an age of 1.3 Gyr (with a range of 0.8–2 Gyr) for ε Indi A based on its rotational properties, and we adopt that age for ε Indi Ba,Bb here. For the median age of 1.3 Gyr, the Baraffe et al. (2003) models predict radii of 0.091 and 0.096 $R_\odot$ for the luminosities of ε Indi Ba and ε Indi Bb, respectively. Assuming $T_{\rm eff} = 5771$ K for the Sun, we then derive $T_{\rm eff} = 1276$ K and 854 K for ε Indi Ba and ε Indi Bb, respectively. The models predict changes of ±5% in the radii across the 0.8–2 Gyr age range, yielding corresponding uncertainties in the effective temperatures of +30/−40 K for ε Indi Ba and ±20 K for ε Indi Bb (see Table 7).

It should be pointed out that Smith et al. (2003) find a significantly higher effective temperature of ∼1500 K for ε Indi Ba based on model atmosphere fitting of high resolution ($R = 50\,000$) near-IR spectra covering lines of CO, H_2O, and CH_4. Contamination in their spectra from the then-unknown ε Indi Bb appears to be minimal. They note that spectroscopically-determined effective temperatures are frequently higher than those calculated using structural models to predict the radius as we have done here, although they offer no explanation why this may be the case. The degree of the disagreement can be illustrated thus. Smith et al. (2003) use their effective temperature along with the published luminosity for ε Indi B of SMLK03 to determine its radius: adjusting for the luminosity derived here for ε Indi Ba alone, we recalculate that radius as 0.061 $R_\odot$, i.e., considerably smaller than the minimum radius of ∼0.085 $R_\odot$ predicted by structural models for low-mass objects at ages 0.8–2 Gyr. Direct measurements of the radius of ε Indi Ba through long-baseline interferometry may help solve this dilemma: at 3.626 pc, 0.085 $R_\odot$ subtends ∼0.25 milliarcsec, challenging but perhaps not impossible (cf. Ségransan et al. 2003).

Finally, we can also use the models to obtain mass estimates for the two T dwarfs. For the luminosity of ε Indi Ba, the Lyon models of Baraffe et al. (2003) yield masses of ∼38–57 $M_{\rm Jup}$ for the range 0.8–2 Gyr, with 47 $M_{\rm Jup}$ for 1.3 Gyr. For reference, the Arizona models (Burrows et al. 1997) yield 42–63 $M_{\rm Jup}$, with 54 $M_{\rm Jup}$ for 1.3 Gyr. For ε Indi Bb, the Lyon models yield 22–35 $M_{\rm Jup}$, with 28 $M_{\rm Jup}$ at 1.3 Gyr; the Arizona models yield 24–38 $M_{\rm Jup}$, with 30 $M_{\rm Jup}$ at 1.3 Gyr. It is important to note that these mass estimates are not significantly affected by the 20% errors in the luminosities: the errors are dominated by the age uncertainty. Even then, the masses are reasonably well constrained: we adopt the Lyon masses of 47 ± 10 $M_{\rm Jup}$ for ε Indi Ba and 28 ± 7 for ε Indi Bb.

5. Discussion

It is evident that ε Indi Ba and ε Indi Bb are very special entries in the growing catalogue of brown dwarfs. They are at a very well-defined distance and have a reasonably well-known age, implying that bolometric luminosities can be measured accurately and then used to determine masses by reference to evolutionary models. The fact that they constitute a binary system means that the distances and ages are the same for both objects, making them a powerful differential probe of these models. To date, only two other T dwarf binaries are known (Burgasser et al. 2003) and neither of these have known ages.

The proximity of ε Indi Ba,Bb to the Sun means that the two components are bright and their relatively large angular

separation implies that detailed physical studies of both sources will be possible, as foreshadowed by the results given in the present paper. At the same time, they are also close enough to each other physically that their orbits can be measured on a reasonable timescale. Assuming masses of 47 and 28 $M_{\rm Jup}$ and a semimajor axis of 2.65 AU, a nominal orbital period of 15.5 years is deduced, although obviously projection effects, orbital eccentricity, and errors in our mass determinations mean that the period could also be either longer or shorter.

The reward for determining the orbit is a model-independent determination of the total system mass, in turn placing strong constraints on the evolutionary models. Of the other two binary T dwarf systems, one (2MASS 1225−2739AB) has a possible period of ∼23 years, while the period of the other (2MASS 1534−2952AB) may be only ∼8 years (Burgasser et al. 2003): however, the latter system is extremely tight with a 0.065 arcsec separation, making it very difficult to obtain separate spectra or accurate astrometry. Luckily, ε Indi Ba,Bb has a a small enough physical separation to help determine its orbit fairly quickly and yet it is close enough to the Sun to allow both components to be well separated. Indeed, if radial velocity variations in the system can also be measured, the individual component masses can also be determined. If the orbit were to lie perpendicular to the plane of sky, a maximum differential radial velocity $\sim 5\,{\rm km\,s^{-1}}$ would be expected. This is readily measurable in principle, although Smith et al. (2003) have found that ε Indi Ba has a high rotational velocity ($v \sin i = 28\,{\rm km\,s^{-1}}$), making it harder in practice.

In any case, ε Indi Ba,Bb will likely prove crucial for an empirical determination of the mass-luminosity relation for substellar objects: accurate, long-term astrometric and radial velocity monitoring of the pair should start as soon as possible.

Finally, it is worth commenting briefly on the announcement of the binary nature of ε Indi B by Volk et al. (2003). They suggested that ε Indi Bb might either be a brown dwarf companion to ε Indi Ba or, alternatively, that ε Indi Bb might be a "large planet". This somewhat provocative latter hypothesis was, however, unsupported even by their own relatively limited data. ε Indi Bb is seen to be only $\sim 1^{\rm m}$ fainter than ε Indi Ba at ~ 1 μm and cursory examination of evolutionary models (e.g., Chabrier et al. 2000) reveals that, at ∼1 Gyr, a 10 $M_{\rm Jup}$ object would be some $4^{\rm m}$–$6^{\rm m}$ fainter than ε Indi Ba at these wavelengths, while a 5 $M_{\rm Jup}$ object would be $>8^{\rm m}$ fainter. Thus it should have been obvious that ε Indi Bb could not be a planet, and indeed, the combined imaging and spectroscopy presented in this paper demonstrate clearly that ε Indi Ba and ε Indi Bb are "just" brown dwarfs, albeit very exciting ones.

Acknowledgements. We would like to thank Chris Lidman, Markus Kasper, Jason Spyromilio, and Roberto Gilmozzi of the VLT on Paranal for their technical and political assistance; Isabelle Baraffe for providing versions of the Baraffe et al. (2003) models for the isochrones appropriate to ε Indi Ba,Bb; Mike Cushing, John Rayner, Ian McLean, Sandy Leggett, Denis Stephens, David Golimowski, Verne Smith, and Ken Hinkle, for communicating and discussing the results of their various papers on T dwarfs prior to publication. We also thank Isabelle Baraffe, Adam Burgasser, Sandy Leggett, Alan MacRobert, Verne Smith, Kevin Volk, Ant Whitworth, Hans Zinnecker, and an anonymous referee for comments which clarified and sharpened various aspects of the submitted paper. MJM thanks the Institute of Astronomy, University of Cambridge, for their valued warm hospitality as this paper was started and finished, and Matthew Bate and Ian Bonnell for doing what they do best; LMC and BB acknowledge support from NASA Origins grant NAGS-12086; and NL thanks the EC Research Training Network "The Formation and Evolution of Young Stellar Clusters" (HPRN-CT-2000-00155) for financial support. This research has made use of data products from the SuperCOSMOS Sky Surveys at the Wide-Field Astronomy Unit of the Institute for Astronomy, University of Edinburgh and from the Two Micron All Sky Survey, which is a joint project of the University of Massachusetts and the Infrared Processing and Analysis Center/California Institute of Technology, funded by the National Aeronautics and Space Administration and the National Science Foundation.

References

Artigau, E., Nadeau, D., & Doyon, R. 2003, in Brown dwarfs, ed. E. Martín (San Francisco: ASP), Proc. IAU Symp., 211, 451
Baraffe, I., Chabrier, G., Barman, T. S., Allard, F., & Hauschildt, P. H. 2003, A&A, 402, 701
Bouy, H., Brandner, W., Martín, E. L., et al. 2003, AJ, 126, 1526
Burgasser, A. J., Kirkpatrick, J. D., Cutri, R. M., et al. 2000, ApJ, 531, L57
Burgasser, A. J., Kirkpatrick, D. J., Brown, M. E., et al. 2002, AJ, 564, 421
Burgasser, A. J., Kirkpatrick, J. D., Reid, I. N., et al. 2003, ApJ, 586, 512
Burrows, A., Marley, M., Hubbard, W. B., et al. 1997, ApJ, 491, 856
Chabrier, G., Baraffe, I., Allard, F., & Hauschildt, P. 2000, ApJ, 542, 464
Close, L. M., Potter, D., Brandner, W., et al. 2002a, ApJ, 566, 1095
Close, L. M., Siegler, N., Freed, M., & Biller, B. 2003, ApJ, 587, 407
Close, L. M., Siegler, N., Potter, D., Brandner, W., & Liebert, J. 2002b, ApJ, 567, L53
Cushing, M. C., Rayner, J. T., Davis, S. P., & Vacca, W. D. 2003, ApJ, 582, 1066
Cutri, R. M., Skrutskie, M. F., van Dyk, S., et al. 2003, 2MASS All-sky Catalog of Point Sources (UMass/IPAC)
Dahn, C. C., Harris, H. C., Vrba, F. J., et al. 2002, AJ, 124, 1170
ESA 1997, Hipparcos and Tycho catalogues, ESA-SP 1200
Geballe, T. R., Knapp, G. R., Leggett, S. K., et al. 2002, AJ, 564, 466
Geballe, T. R., Kulkarni, S. R., Woodward, C. E., & Sloan, G. C. 1996, ApJ, 467, L101
Geballe, T. R., Saumon, D., Leggett, S. K., et al. 2001, ApJ, 556, 373
Gizis, J. E., Reid, I. N., Knapp, G. R., et al. 2003, AJ, 125, 3302
Golimowski, D. A., et al. 2004, AJ, submitted
Goto, M., Kobayashi, N., Terada, H., et al. 2002, ApJ, 567, L59
Hambly, N. C., Irwin, M. J., & MacGillivray, H. T. 2001a, MNRAS, 326, 1295
Hambly, N. C., MacGillivray, H. T., Read, M. A., et al. 2001b, MNRAS, 326, 1279
Hartkopf, W. I., & Mason, B. D. 2003, `http://ad.usno.navy.mil/wds/wmc/wmc_post191.html`
Lachaume, R., Dominik, C., Lanz, T., & Habing, H. J. 1999, A&A, 348, 897
Lagrange, A.-M., Chauvin, G., Fusco, T., et al. 2003, in Instrument design and 2003, performance for optical/infrared ground-based telescopes, ed. M. Iye, & A. F. Moorwood, Proc. SPIE, 4841, 860
Leggett, S. K., Golimowski, D. A., Fan, X., et al. 2002, ApJ, 564, 452

Lenzen, R., Hartung, M., Brandner, W., et al. 2003, in Instrument design and performance for optical/infrared ground-based telescopes, ed. M. Iye & A. F. Moorwood, Proc. SPIE, 4841, 944
Maiolino, R., Rieke, G. H., & Rieke, M. J. 1996, AJ, 111, 537
Martín, E. L., Brandner, W., & Basri, G. 1999, Science, 283, 1718
McLean, I. S., McGovern, M. R., Burgasser, A. J., et al. 2003, ApJ, 596, 561
Nakajima, T., Oppenheimer, B. R., Kulkarni, S. R., et al. 1995, Nature, 378, 463
Potter, D., Martín, E. L., Cushing, M. C., et al. 2002, ApJ, 567, L133
Reid, I. N., Gizis, J. E., Kirkpatrick, J. D., & Koerner, D. W. 2001, AJ, 121, 498
Scholz, R.-D., McCaughrean, M. J., Lodieu, N., & Kuhlbrodt, B. 2003, A&A, 389, L29 (SMLK03)
Ségransan, D., Kervella, P., Forveille, T., & Queloz, D. 2003, A&A, L5
Smith, V. V., Tsuji, T., Hinkle, K. H., et al. 2003, ApJL, in press
Stephens, D. C., & Leggett, S. K. 2004, PASP, in press
Tinney, C. G., Burgasser, A. J, & Kirkpatrick, J. D. 2003, AJ, 126, 975
Volk, K., Blum, R., Walker, G., & Puxley, P. 2003, IAU Circ., 8188, 2